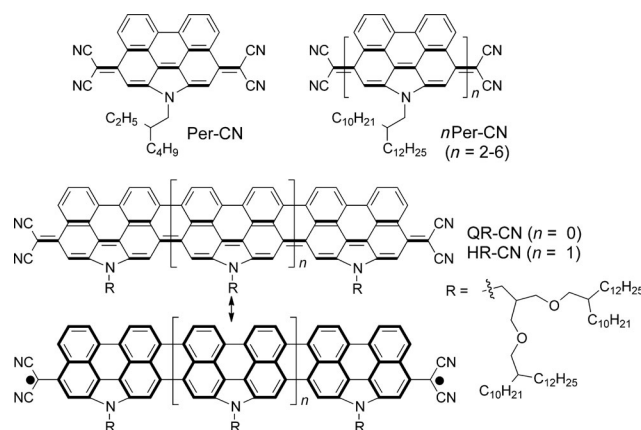


# Tetracyanoquaterrylene and Tetracyanohexarylenequinodimethanes with Tunable Ground States and Strong Near-Infrared Absorption\*\*

Zebing Zeng, Sangsu Lee, José L. Zafra, Masatoshi Ishida, Xiaojian Zhu, Zhe Sun, Yong Ni, Richard D. Webster, Run-Wei Li, Juan T. López Navarrete,\* Chunyan Chi,\* Jun Ding,\* Juan Casado,\* Dongho Kim,\* and Jishan Wu\*

Recently, there has been increasing interest in singlet open-shell polycyclic hydrocarbons,<sup>[1]</sup> which possess unique optical, electronic, and magnetic properties for potential applications in organic electronics,<sup>[2]</sup> non-linear optics,<sup>[3]</sup> spintronics,<sup>[4]</sup> and energy storage devices.<sup>[5]</sup> A general design is to embed a quinoidal unit such as *p*-quinodimethane (*p*-QDM), 2,6-naphthoquinodimethane and 2,6-anthraquinodimethane into a polycyclic hydrocarbon framework, and the obtained hydrocarbons can show a singlet biradical nature owing to the recovery of aromaticity of the proaromatic subunit and the spin-polarization at the terminal carbon atoms. With diverse synthetic approaches, numerous examples of this type of hydrocarbons, including bisphenalenyls,<sup>[6]</sup> indenofluorenes,<sup>[7]</sup> and zethrenes<sup>[8]</sup> have been developed as open-shell biradical species. In addition, zigzag-edged nanographenes, such as higher-order acenes,<sup>[9]</sup> periacenes,<sup>[10]</sup> and anthenes,<sup>[11]</sup> can show a singlet biradical ground state owing to the gain of additional aromatic sextet rings in the biradical form. Moreover, quinoidal hydrocarbons embedded with  $\pi$ -extended *p*-QDM structure,<sup>[12]</sup> quinoidal oligothiophenes,<sup>[13]</sup> and quinoidal porphyrins and its dimers<sup>[14]</sup> are intriguing in view of their unique chemical and physical properties.

We recently have synthesized a series of tetracyano-oligo(*N*-annulated perylene (NP)) quinodimethanes (Per-CN and *n*Per-CN, *n* = 2–6, Figure 1) as soluble and stable  $\pi$ -extended *p*-QDMs.<sup>[15]</sup> The smallest member of this series, Per-



**Figure 1.** Chemical structures of Per-CN, *n*Per-CN, QR-CN, and the two resonance structures of HR-CN.

CN, has a closed-shell quinoidal structure, while the longer oligomers all exhibit a ground-state biradicaloid character. The chain-length dependent physical properties (for example, magnetic, optical, electronic) lead us to prepare new oligomeric quinoidal derivatives containing fully fused NP units for a systematic investigation of the structural effect on the open-shell biradical nature of  $\pi$ -extended quinodimethanes. In this study, the tetracyanoquaterrylenequinodimethane (QR-CN)

[\*] Dr. Z. Zeng, Z. Sun, Y. Ni, Prof. C. Chi, Prof. J. Wu  
Department of Chemistry, National University of Singapore  
3 Science Drive 3, 117543, Singapore (Singapore)  
E-mail: chmcc@nus.edu.sg  
chmwuj@nus.edu.sg

S. Lee, Dr. M. Ishida, Prof. D. Kim  
Department of Chemistry, Yonsei University  
Seoul 120-749 (Korea)  
E-mail: dongho@yonsei.ac.kr

J. L. Zafra, Prof. J. T. López Navarrete, Prof. J. Casado  
Department of Physical Chemistry, University of Malaga  
Campus de Teatinos s/n 229071 Malaga (Spain)  
E-mail: teodomiro@uma.es  
casado@uma.es

X. Zhu, Prof. R.-W. Li  
Key Laboratory of Magnetic Materials and Devices  
Ningbo Institute of Materials Technology and Engineering  
Chinese Academy of Sciences, Ningbo 315201 (China)  
Prof. R. D. Webster  
Division of Chemistry & Biological Chemistry  
School of Physical & Mathematical Sciences

Nanyang Technological University  
21 Nanyang Link, 637371, Singapore (Singapore)

Prof. J. Ding  
Department of Materials Science & Engineering  
National University of Singapore, 119260 (Singapore)  
E-mail: msedingj@nus.edu.sg

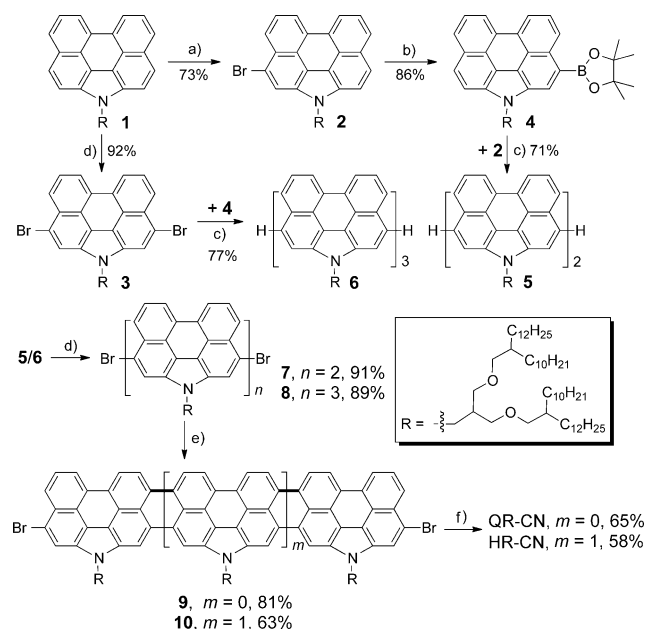
Prof. J. Wu  
Institute of Materials Research and Engineering, A\*STAR  
3 Research Link, 117602, Singapore (Singapore)

[\*\*] J.W. acknowledges the financial support from MOE Tier 2 grant (MOE2011-T2-2-130) and IMRE Core funding. The work at Yonsei Univ. was supported by WCU programs (R32-2010-10217-0) and an AFSOR/APARD grant (no. FA2386-09-1-4092). The work at Spain was supported by the Ministerio de Educación y Ciencia of Spain and by FEDER funds.

Supporting information for this article is available on the WWW under <http://dx.doi.org/10.1002/anie.201305348>.

and tetracyanohexarylenequinodimethane (HR-CN), with highly planar fused structures, were synthesized, and their ground-state electronic properties were investigated by various steady-state and time-resolved spectroscopic techniques and magnetic susceptibility measurements (Figure 1). Understanding the electronic structures of QR-CN and HR-CN would be of importance to extract information about the steric effect on the biradical resonance contribution by comparison with non-fused derivatives (that is, 2Per-CN and 3Per-CN). The dihedral angles between the rylene units in *n*Per-CN were dependent on the distinct biradical character ( $\gamma$ ). Therefore the fully fused quinodimethane cores in QR-CN and HR-CN would be informative derivatives to evaluate the nature of chemical bonding characters. Furthermore, the rylene derivatives belong to an important family of organic dyes,<sup>[16]</sup> and therefore the largely extended  $\pi$ -conjugation in quinoidal QR-CN and HR-CN would result in a small energy gap, giving a strong electronic absorption in the near-infrared (NIR) region.

Synthesis of  $\pi$ -extended quinoidal rylenes horizontally longer than perylenes is still a challenging subject because of the intrinsic chemical instability. Furthermore, the intramolecular C–C bond formation between adjacent rylene units either by oxidative cyclodehydrogenation<sup>[16,17]</sup> or by base-mediated Michael addition followed by aromatization in air is a difficult step.<sup>[16,18]</sup> Our initial attempts of direct intramolecular cyclization of *n*Per-CN by using various oxidants (for example, FeCl<sub>3</sub> or DDQ/Sc(OTf)<sub>3</sub>) or bases all gave complicated mixtures. Therefore, we have changed the strategy by using Takahashi cross-coupling<sup>[19]</sup> reaction of the pre-constructed fused quaterylene (**9**) and hexarylene (**10**) dibromide precursors with malononitrile (Scheme 1). A



**Scheme 1.** Reagents and conditions: a) NBS (1 equiv), CH<sub>2</sub>Cl<sub>2</sub>, 0 °C; b) pinacolborane, [PdCl<sub>2</sub>(PPh<sub>3</sub>)<sub>2</sub>], 1,2-dichloroethane/Et<sub>3</sub>N, 90 °C; c) [Pd(PPh<sub>3</sub>)<sub>4</sub>], Cs<sub>2</sub>CO<sub>3</sub>, toluene/DMF, 90 °C; d) NBS (2 equiv), CH<sub>2</sub>Cl<sub>2</sub>/DMF, 0–25 °C; e) DDQ/Sc(OTf)<sub>3</sub>, toluene, reflux; f) i) malononitrile, NaH, [Pd(PPh<sub>3</sub>)<sub>2</sub>Cl<sub>2</sub>], reflux; ii) HCl (2 M), 0–5 °C.

highly branched aliphatic ether substituent at the *N*-position (for details of the synthesis, see the Supporting Information) was used to ensure sufficient solubility of both the intermediate compounds (**9** and **10**) and the final products.<sup>[20]</sup> The dibromo- NP dimer **5** and trimer **6** were prepared by stepwise coupling reactions starting from the monomer **1**. Bromination of **5** and **6** by NBS gave the dibromo- NP dimer **7** and trimer **8**, respectively, in high yields. The key intermediates **9** and **10** were successfully prepared by oxidative cyclodehydrogenation of the corresponding precursors **7** and **8** with DDQ/Sc(OTf)<sub>3</sub>.<sup>[17,18]</sup> The absorption spectra of **9** and **10** are similar to those of the previously reported *N*-annulated quaterylene<sup>[18]</sup> and hexarylene,<sup>[17]</sup> respectively (Supporting Information, Figure S1). The longer fused rylenes (for example, dibromooctarylene) were not obtained under the same conditions because of the difficulty in purification of the crude product (containing incomplete reaction products). Subsequent Takahashi coupling of **9** and **10** with malononitrile followed by simultaneous oxidation in air afforded the desired products QR-CN and HR-CN. These products were carefully purified by column chromatography followed by preparative thin-layer chromatography. The purity of the final products was confirmed by high-resolution MALDI mass spectrometry and high performance liquid chromatography (see the Supporting Information).

The electronic structures of QR-CN and HR-CN were investigated by a combination of electron spin resonance (ESR), a superconducting quantum interference device (SQUID), and Raman spectroscopy as well as the density functional theory (DFT) calculations. The solid-state EPR spectra of QR-CN exhibited no active signals, though no clear <sup>1</sup>H NMR spectrum of QR-CN was obtained, which is presumably due to the strong aggregation in solution. This implies a closed-shell ground state structure of QR-CN. In contrast, a broad ESR signal with a *g*-tensor of *g<sub>e</sub>* = 2.0029 recorded at 153 K suggested an existence of open-shell species in HR-CN, as seen in the non-fused 3Per-CN (Supporting Information, Figure S2).<sup>[15]</sup> Accordingly, the temperature-dependent magnetic susceptibility behaviors of HR-CN (5–380 K) obtained by SQUID measurements revealed that HR-CN has a singlet biradical electronic structure in the ground state (Supporting Information, Figure S3). Upon careful fitting of the plots by using the Bleaney–Bowers equation,<sup>[21]</sup> the exchange interaction,  $2J/k_B$  was estimated to be –2120 K. The singlet–triplet energy gap ( $\Delta E_{\text{SB-TB}}$ ) of about 4.21 kcal mol<sup>–1</sup> was found to be significantly larger than that of 3Per-CN (0.107 kcal mol<sup>–1</sup>).

To get further insights on the shape of the electronic ground state, resonant Raman spectra<sup>[12,13c,15,22]</sup> were recorded for Per-CN, QR-CN, and HR-CN (Figure 2A) with laser excitations at 532, 785, and 1064 nm, respectively, which coincide with their most intense Vis-NIR electronic absorptions in Figure 3. The most intense bands of Per-CN (1705, 1594, and 1458 cm<sup>–1</sup>) are typical markers for closed-shell quinoidal structure. On passing to QR-CN, some of these Raman bands experience a simultaneous frequency downshift and splitting, that is, the 1705 and 1594 cm<sup>–1</sup> bands evolved into the 1700/1659 cm<sup>–1</sup> and 1582/1566 cm<sup>–1</sup> pairs, respectively. At the same time, two new bands appeared at 1536 and

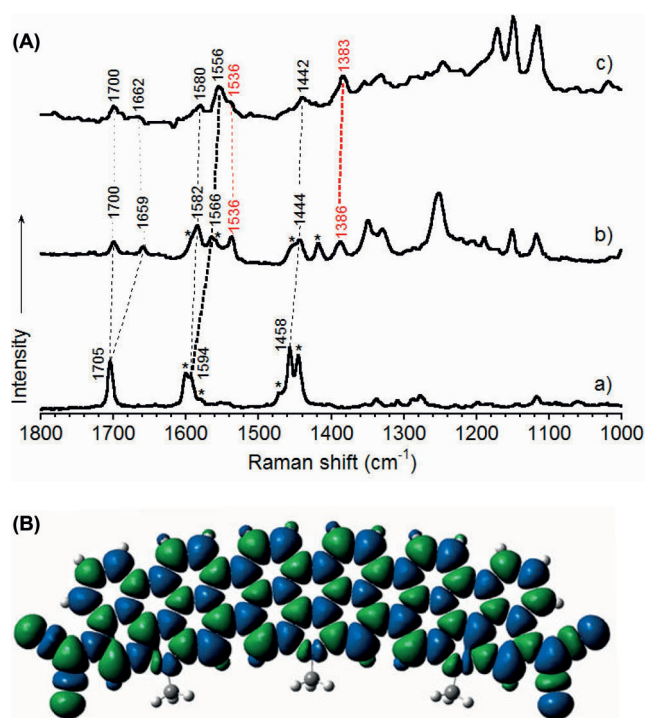


**Figure 2.** A) Solid-state resonant Raman spectra of a) Per-CN ( $\lambda_{\text{exc}} = 532$  nm), b) QR-CN ( $\lambda_{\text{exc}} = 785$  nm), and c) HR-CN ( $\lambda_{\text{exc}} = 1064$  nm). Asterisks denote bands that do not change within the series. B) Calculated (UCAM-B3LYP/6-31G(d,p)) spin-density distribution of HR-CN (singlet biradical, the methyl group was used for the N-substituents); the blue and green surfaces represent  $\alpha$  and  $\beta$  spin densities, respectively.

$1386\text{ cm}^{-1}$ , which are likely associated with the new bonds planarizing the NP units. The frequency downshift of the  $\nu_s(\text{C}=\text{C})$  modes might result from: 1) increased conjugation that is due to the increment of  $\pi$ -electrons, which relaxes the bond length alternation path; and 2) an aromatization of the quinoidal benzenes owing to the gaining of biradical character which also weakens the inter-rylene CC bonds. On passing to HR-CN, the most intense Raman bands are those at  $1556\text{ cm}^{-1}$  ( $1594\text{ cm}^{-1}$  in Per-CN and  $1566\text{ cm}^{-1}$  in QR-CN) and at  $1383\text{ cm}^{-1}$  ( $1386\text{ cm}^{-1}$  in QR-CN), the latter revealing a further weakening of the inter-rylene C–C bonds upon QR-CN  $\rightarrow$  HR-CN. The bands at  $1386\text{ cm}^{-1}$  and  $1383\text{ cm}^{-1}$  in QR-CN and HR-CN are related with those at  $1378\text{ cm}^{-1}$  in 2Per-CN and  $1343\text{ cm}^{-1}$  in 3Per-CN. We have interpreted the frequencies of these Raman modes as indicative of a medium open-shell character for 2Per-CN and a large open-shell character for 3Per-CN both with a singlet biradical ground state.<sup>[15]</sup> This comparison reveals that: 1) QR-CN and HR-CN both have singlet ground electronic states; and 2) the relative weights of the open-shell property are expressed as follows: QR-CN < 2Per-CN, HR-CN < 3Per-CN, and HR-CN  $\leq$  2Per-CN. Summing up, HR-CN has a higher singlet open-shell character than QR-CN but still moderate and not comparable to that of 3Per-CN. This spectroscopic finding can be interpreted in terms of double-spin polarization, which favors the singlet open-shell form versus the triplet owing to preferred conjugation of the unpaired electrons in the singlet

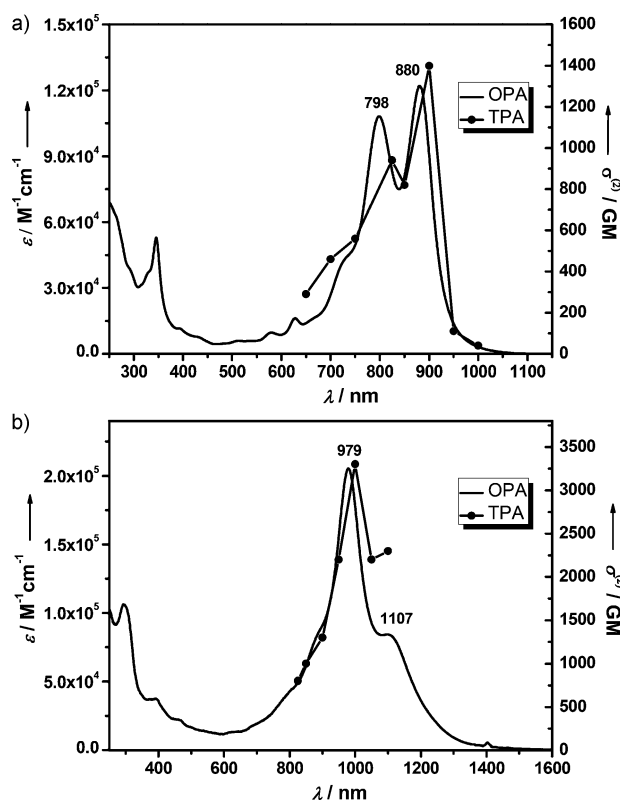


**Figure 3.** OPA spectra (left vertical axis) and TPA spectra (right vertical axis) of (a) QR-CN and (b) HR-CN in toluene. TPA spectra are plotted at  $\lambda_{\text{ex}}/2$ .

format, which causes an enlargement of the singlet–triplet energy gap. In our case, the planar structure of the oligorylene would certainly favor conjugation, which would enlarge the singlet–triplet gap and reduce the open-shell character. In contrast, for 2Per-CN and 3Per-CN, the large steric repulsion between the NP units drives the molecules into a much more accentuated open-shell biradical state.

On the basis of these experimental findings, unrestricted broken-symmetry DFT (UCAM-B3LYP/6-31G(d,p)) calculations were carried out for a better understanding of the ground state of open-shell HR-CN. The optimized geometry of HR-CN demonstrated the highly planar core with a curved quinoidal backbone restricted by *N*-fusion of five-membered rings (Supporting Information, Figure S4). The molecular orbital profiles of the singlet biradical state of HR-CN exhibit a characteristic disjoint feature as seen in the singlet biradical molecules.<sup>[12,13c,15,22]</sup> The spin electrons are delocalized over the whole  $\pi$ -framework (Figure 2B; Supporting Information, Figure S5). The theoretically predicted singlet–triplet energy gap ( $\Delta E_{\text{SB-TB}}$ ) is  $6.02\text{ kcal mol}^{-1}$ , which is well correlated with the experimentally determined value (see above).<sup>[23]</sup> The singlet biradical character ( $y$ ) of HR-CN was determined to be 0.064 by using CASSCF(2,2)/6-31G calculation. Compared to that of non-fused 3Per-CN, the fact that HR-CN has a larger singlet–triplet energy gap and a smaller biradical index indicates the core geometry should be responsible for the degree of biradical nature. The dihedral angle between the rylene cores would be one of the critical factors for fine-

tuning the electronic configuration of quinoidal molecules. The restricted CAM-B3LYP calculation for QR-CN and Per-CN produced the similar planar geometries to that of HR-CN. Analyses on the calculated bond lengths and the nucleus independent chemical shift (NICS) values (for example, NICS(1) and NICS(1)<sub>zz</sub>) reveal that more aromatic benzenoid characters of the six-membered rings of the rylene moieties are seen as prolonging the molecular lengths from Per-CN, QR-CN to HR-CN (Supporting Information, Figures S6 and S7). This feature supports that the recovery of the aromaticity is the major driving force for the increased singlet biradical character.

Along with the different electronic structures, the characteristic optical properties of the fused quinoidal rylenes were realized in the one-photon absorption (OPA) and two-photon absorption (TPA) spectra of QR-CN and HR-CN (Figure 3). QR-CN has a green color in dichromethane solution, and its absorption spectrum revealed quite similar spectral feature to that of Per-CN but showed a remarkable red-shift of the band (approximately 254 nm) with a drastic increase of the extinction coefficient ( $\epsilon = 1.2 \times 10^5 \text{ L mol}^{-1} \text{ cm}^{-1}$  for QR-CN and  $6.6 \times 10^4 \text{ L mol}^{-1} \text{ cm}^{-1}$  for Per-CN). This supports the notion that QR-CN has a closed-shell quinoidal structure in the ground state, the same as Per-CN. The time-dependent (TD) DFT stick spectra of closed shell QR-CN and Per-CN are consistent with this conclusion (Supporting Information, Figure S8). In a sharp contrast, the OPA spectrum of HR-CN displays characteristic optical features; the intense band at 979 nm ( $\epsilon = 2.1 \times 10^5 \text{ L mol}^{-1} \text{ cm}^{-1}$ ) together with a shoulder at longer wavelength (1107 nm) was observed. The narrower optical HOMO–LUMO gap was estimated to be 0.97 eV, and the lowest energy absorption band structures were identified by TD-DFT calculation approach as admixing the doubly excited electronic configuration  $^1\Phi_{\text{H,H} \rightarrow \text{L,L}}$  into the ground state (Supporting Information, Figure S8).<sup>[24]</sup> This result is consistent with that HR-CN is a ground singlet biradical species. It is also worthy to note that due to negligible absorption in the visible region (400–700 nm), HR-CN is almost colorless in solution, thus it represents a rare organic dye with very strong NIR absorption but transparent in visible spectral window. This finding would meet up with the technological applications, such as for security printing.

The excited electronic properties of fused quinoids, QR-CN and HR-CN, were analyzed by time-resolved optical spectroscopy. Interestingly, the singlet excited lifetimes of the series of quinoids were found to increase upon extension of the rylene cores (Per-CN (17 ps)<sup>[15]</sup> < QR-CN (24 ps) < HR-CN (29 ps)) by femtosecond transient absorption measurement, albeit their larger molecular sizes (Supporting Information, Figure S9). This is an opposite trend to those of Per-CN species, which may imply that the recovery of the aromatic rylene cores especially in HR-CN would contribute to their excited state dynamics.

The intermediate singlet biradical character ( $0 < y < 1$ ) is known as a diagnostic parameter that enhances nonlinear optical responses in open-shell biradical molecules.<sup>[3]</sup> The two-photon absorption (TPA) measurements for Per-CN, QR-CN, and HR-CN were conducted in toluene in the NIR

region from 1300 to 2200 nm where one-photon absorption contribution is negligible (Figure 3; Supporting Information, Figure S10). QR-CN exhibited a  $\sigma_{\text{max}}^{(2)} = 1400 \text{ GM}$  at 1800 nm which is slightly larger than Per-CN ( $\sigma_{\text{max}}^{(2)} = 1300 \text{ GM}$  at 1200 nm). In particular, the significantly larger value of  $\sigma_{\text{max}}^{(2)} = 3300 \text{ GM}$  excited at 2000 nm for HR-CN was observed compared to that of 3Per-CN ( $\sigma_{\text{max}}^{(2)} = 770 \text{ GM}$ )<sup>[15]</sup> despite smaller singlet indices of 0.06 for HR-CN (vs 0.99 for 3Per-CN). This could be due to the extended conjugation induced by increased rigidity of HR-CN, which greatly enhances the second hyperpolarizability and improves the third-order optical nonlinearity including the TPA performance.<sup>[25]</sup>

QR-CN showed amphoteric redox behavior with three oxidation processes at  $E_{1/2}^{\text{ox}} = 0.18, 0.36, 0.84 \text{ V}$  and four reduction waves at  $E_{1/2}^{\text{red}} = -0.87, -0.97, -1.50, -2.15 \text{ V}$  (vs  $\text{Fc}/\text{Fc}^+$ ,  $\text{Fc} = \text{ferrocene}$ ) in cyclic voltammetry and differential pulse voltammetry experiments (Supporting Information, Figure S11). In contrast, Per-CN does not show any detectable oxidation waves,<sup>[15]</sup> indicating that the larger extended  $\pi$  system in QR-CN can stabilize multiple positive/negative charges. The HOMO and LUMO energy levels were determined to be  $-4.83$  and  $-4.03 \text{ eV}$ , respectively, from the onset potentials of the first oxidation and reduction waves. Unfortunately, HR-CN did not exhibit the well-resolved redox waves possibly due to intrinsically strong  $\pi$ – $\pi$  stacking between the highly planar hexarylene cores.

In summary, two new soluble and stable quinoidal rylene molecules QR-CN and HR-CN were successfully prepared. With extension of the rylene core size, the ground state electronic structures of these quinoidal derivatives are changed from a closed-shell singlet for Per-CN and QR-CN to an open-shell singlet biradical for HR-CN. As being different from the non-fused oligomeric rylenes (that is, 2Per-CN and 3Per-CN), QR-CN and HR-CN showed very strong OPA and TPA response in the NIR range owing to the extended  $\pi$ -conjugation as well as the appropriate singlet biradical character. Our research demonstrated that stable, highly extended quinoidal polycyclic hydrocarbons can be achieved by rational design and appropriate synthetic strategy, which leads to new opportunities to develop new NIR chromophores and semiconductors for photonics, electronics and spintronics.

Received: June 21, 2013

Published online: July 23, 2013

**Keywords:** biradicaloids · hexarylene · near-infrared dyes · polycyclic hydrocarbons · quaterylene

- [1] a) C. Lambert, *Angew. Chem.* **2011**, *123*, 1794–1796; *Angew. Chem. Int. Ed.* **2011**, *50*, 1756–1758; b) Y. Morita, K. Suzuki, S. Sato, T. Takui, *Nat. Chem.* **2011**, *3*, 197–204; c) Z. Sun, Q. Ye, C. Chi, J. Wu, *Chem. Soc. Rev.* **2012**, *41*, 7857–7889; d) A. Shimizu, Y. Hirao, T. Kubo, M. Nakano, E. Botek, B. Champagne, *AIP Conf. Proc.* **2012**, *1504*, 399–405.
- [2] a) M. Chikamatsu, T. Mikami, J. Chisaka, Y. Yoshida, R. Azumi, K. Yase, *Appl. Phys. Lett.* **2007**, *91*, 043506; b) D. T. Chase, A. G. Fix, S. J. Kang, B. D. Rose, C. D. Weber, Y. Zhong, L. N.



- Zakharov, M. C. Lonergan, C. Nuckolls, M. M. Haley, *J. Am. Chem. Soc.* **2012**, *134*, 10349–10352.
- [3] K. Kamada, K. Ohta, T. Kubo, A. Shimizu, Y. Morita, K. Nakasuji, R. Kishi, S. Ohta, S. I. Furukawa, H. Takahashi, M. Nakano, *Angew. Chem.* **2007**, *119*, 3614–3616; *Angew. Chem. Int. Ed.* **2007**, *46*, 3544–3546.
- [4] Y. W. Son, M. L. Cohen, S. G. Louie, *Phys. Rev. Lett.* **2006**, *97*, 216803.
- [5] Y. Morita, S. Nishida, T. Murata, M. Moriguchi, A. Ueda, M. Satoh, K. Arifuku, K. Sato, T. Takui, *Nat. Mater.* **2011**, *10*, 947–951.
- [6] a) K. Ohashi, T. Kubo, T. Masui, K. Yamamoto, K. Nakasuji, T. Takui, Y. Kai, I. Murata, *J. Am. Chem. Soc.* **1998**, *120*, 2018–2027; b) T. Kubo, M. Sakamoto, M. Akabane, Y. Fujiwara, K. Yamamoto, M. Akita, K. Inoue, T. Takui, K. Nakasuji, *Angew. Chem.* **2004**, *116*, 6636–6641; *Angew. Chem. Int. Ed.* **2004**, *43*, 6474–6479; c) A. Shimizu, T. Kubo, M. Uruichi, K. Yakushi, M. Nakano, D. Shiomi, K. Sato, T. Takui, Y. Hirao, K. Matsumoto, H. Kurata, Y. Morita, K. Nakasuji, *J. Am. Chem. Soc.* **2010**, *132*, 14421–14428; d) A. Shimizu, Y. Hirao, K. Matsumoto, H. Kurata, T. Kubo, M. Uruichi, K. Yakushi, *Chem. Commun.* **2012**, *48*, 5629–5631.
- [7] a) D. T. Chase, B. D. Rose, S. P. McClintock, L. N. Zakharov, M. M. Haley, *Angew. Chem.* **2011**, *123*, 1159–1162; *Angew. Chem. Int. Ed.* **2011**, *50*, 1127–1130; b) A. Shimizu, R. Kishi, M. Nakano, D. Shiomi, K. Sato, T. Takui, I. Hisaki, M. Miyata, Y. Tobe, *Angew. Chem.* **2013**, *125*, 6192–6195; *Angew. Chem. Int. Ed.* **2013**, *52*, 6076–6079.
- [8] a) R. Umeda, D. Hibi, K. Miki, Y. Tobe, *Org. Lett.* **2009**, *11*, 4104–4106; b) T. C. Wu, C. H. Chen, D. Hibi, A. Shimizu, Y. Tobe, Y. T. Wu, *Angew. Chem.* **2010**, *122*, 7213–7216; *Angew. Chem. Int. Ed.* **2010**, *49*, 7059–7062; c) Z. Sun, K.-W. Huang, J. Wu, *Org. Lett.* **2010**, *12*, 4690–4693; d) Z. Sun, K.-W. Huang, J. Wu, *J. Am. Chem. Soc.* **2011**, *133*, 11896–11899; e) Y. Li, W.-K. Heng, B. S. Lee, N. Aratani, J. L. Zafra, N. Bao, R. Lee, Y. M. Sung, Z. Sun, K.-W. Huang, R. D. Webster, J. T. López Navarrete, D. Kim, A. Osuka, J. Casado, J. Ding, J. Wu, *J. Am. Chem. Soc.* **2012**, *134*, 14913–14922.
- [9] M. Bendikov, H. M. Duong, K. Starkey, K. N. Houk, E. A. Carter, F. Wudl, *J. Am. Chem. Soc.* **2004**, *126*, 7416–7417.
- [10] D. E. Jiang, B. G. Sumpter, S. Dai, *J. Chem. Phys.* **2007**, *127*, 124703.
- [11] a) A. Konishi, Y. Hirao, M. Nakano, A. Shimizu, E. Botek, B. Champagne, D. Shiomi, K. Sato, T. Takui, K. Matsumoto, H. Kurata, T. Kubo, *J. Am. Chem. Soc.* **2010**, *132*, 11021–11023; b) A. Konishi, Y. Hirao, K. Matsumoto, H. Kurata, R. Kishi, Y. Shigeta, M. Nakano, K. Tokunaga, K. Kamada, T. Kubo, *J. Am. Chem. Soc.* **2013**, *135*, 1430–1437.
- [12] a) Z. Zeng, Y. M. Sung, N. Bao, D. Tan, R. Lee, J. L. Zafra, B. S. Lee, M. Ishida, J. Ding, J. T. López Navarrete, Y. Li, W. Zeng, D. Kim, K.-W. Huang, R. D. Webster, J. Casado, J. Wu, *J. Am. Chem. Soc.* **2012**, *134*, 14513–14525; b) X. Zhu, H. Tsuji, K. Nakabayashi, S. Ohkoshi, E. Nakamura, *J. Am. Chem. Soc.* **2011**, *133*, 16342–16345.
- [13] a) J. Casado, R. P. Ortiz, J. T. López Navarrete, *Chem. Soc. Rev.* **2012**, *41*, 5672–5686; b) T. Takahashi, K. I. Matsuoka, K. Takimiya, T. Otsubo, Y. Aso, *J. Am. Chem. Soc.* **2005**, *127*, 8928–8929; c) R. P. Ortiz, J. Casado, V. Hernandez, J. T. López Navarrete, P. M. Viruela, E. Orti, K. Takimiya, T. Otsubo, *Angew. Chem.* **2007**, *119*, 9215–9219; *Angew. Chem. Int. Ed.* **2007**, *46*, 9057–9061.
- [14] a) I. M. Blake, H. L. Anderson, D. Beljonne, J. L. Brédas, W. Clegg, *J. Am. Chem. Soc.* **1998**, *120*, 10764–10765; b) I. M. Blake, A. Krivokapic, M. Katterle, H. L. Anderson, *Chem. Commun.* **2002**, 1662–1663; c) W. D. Zeng, B. S. Lee, Y. M. Sung, K.-W. Huang, Y. Li, D. Kim, J. Wu, *Chem. Commun.* **2012**, *48*, 7684–7686.
- [15] Z. Zeng, M. Ishida, J. L. Zafra, X. Zhu, Y. M. Sung, N. Bao, R. D. Webster, B. S. Lee, R.-W. Li, W. Zeng, Y. Li, C. Chi, J. T. López Navarrete, J. Ding, J. Casado, D. Kim, J. Wu, *J. Am. Chem. Soc.* **2013**, *135*, 6363–6371.
- [16] a) T. Weil, T. Vosch, J. Hofkens, K. Peneva, K. Müllen, *Angew. Chem.* **2010**, *122*, 9252–9278; *Angew. Chem. Int. Ed.* **2010**, *49*, 9068–9093; b) N. G. Pschirer, C. Kohl, F. Nolde, J. Qu, K. Müllen, *Angew. Chem.* **2006**, *118*, 1429–1432; *Angew. Chem. Int. Ed.* **2006**, *45*, 1401–1404.
- [17] Y. Li, J. Gao, S. D. Motta, F. Negri, Z. Wang, *J. Am. Chem. Soc.* **2010**, *132*, 4208–4213.
- [18] C. Jiao, K.-W. Huang, J. Luo, J. Wu, *Org. Lett.* **2009**, *11*, 4508–4511.
- [19] M. Uno, K. Seto, M. Masuda, W. Ueda, S. Takahashi, *Tetrahedron Lett.* **1985**, *26*, 1553–1556.
- [20] An analogue of **9** with the *N*-2-decyltetradecyl substitution (same as the *n*Per-CN) showed much less solubility, which hampered the subsequent Takahashi coupling reaction.
- [21] B. Bleaney, K. D. Bowers, *Proc. R. Soc. London Ser. A* **1952**, *214*, 451–465.
- [22] a) J. Casado, S. Patchkovskii, M. Z. Zgierski, L. Hermosilla, C. Sieiro, M. M. Oliva, J. T. López Navarrete, *Angew. Chem.* **2008**, *120*, 1465–1468; b) *Angew. Chem. Int. Ed.* **2008**, *47*, 1443–1446; S. R. González, Y. Ie, Y. Aso, J. T. López Navarrete, J. Casado, *J. Am. Chem. Soc.* **2011**, *133*, 16350–16353.
- [23] The relatively larger energy difference (ca. 2 kcal mol<sup>-1</sup>) between the calculation and experimental values can be ascribed to the wavefunctional contribution by the overestimation for a larger  $\pi$ -conjugated open-shell system as well as the technical fitting errors resulting from the smaller magnetic susceptibility signal in the SQUID measurement.
- [24] S. Di Motta, F. Negri, D. Fazzi, C. Castiglioni, E. V. Canesi, *J. Phys. Chem. Lett.* **2010**, *1*, 3334–3339.
- [25] K. S. Kim, J. M. Lim, A. Osuka, D. Kim, *J. Photochem. Photobiol. C* **2008**, *9*, 13–28.